

No. LXXXII, DECEMBRIS MMXXIV

ISSN: 2001-9734

ISBN: 978-91-89979-24-6

# ACTA ACADEMIAE STROMSTADIENSIS

**Angelika Basch**



**Perovskite Solar Cell Research Lab Course for Higher  
Science Education**

# Perovskite Solar Cell Research Lab Course for Higher Science Education

Angelika Basch <sup>a,b,\*</sup>)

<sup>a)</sup> University of Applied Sciences Upper Austria, Stelzhammerstrasse 28, 4600 Wels, Austria

<sup>b)</sup> Strömstad Academy, SE-45280 Strömstad, Sweden

angelika@basch.at

## Abstract

This paper summarizes the preliminary results of an on-going higher-education lab course on perovskite solar cell research. The project is planned on a small budget (less than 1000€ per year) for undergraduate engineering students and aims to prepare and characterise perovskite solar cells with no major adaptations such as inert gas techniques. A two-step deposition process, using low-cost materials such as copper thiocyanate (CuSCN) as hole transport material is pursued utilising a routine teaching lab, and in-house built or improvised lab equipment such as a spin coater, a vacuum vessel or a sun simulator and solar cell characterisation test equipment. During the course students are able to discuss their results with active researchers in the field and adjust their own research approach through the access to latest results and ideas. The course serves as training for undergraduate engineering students in photovoltaics and its emerging technologies, basic chemistry skills, material science, project management, presentation methods (such as presentations, posters and videos) characterisation methods such as scanning electron microscopy (SEM), and solar cell characterisation and to conceptualise research projects while manufacturing perovskite solar cells from scratch on a low budget and with basic infrastructure.

Key words: photovoltaics, solar cells, perovskite, higher education, lab course, science education

## 1 Introduction

Perovskite solar cells are an emerging and promising photovoltaics technology. They have first been described in the beginning of 2009 when Kojima *et al.* [1] reported 3.8% efficiency solar cells prepared with simple wet chemistry and a production temperature not exceeding 500°C. In 2024 perovskite solar cells have reached 26.1% efficiency [2]. Several commercial start-ups have been founded. Currently, the research focus is on perovskite on silicon tandems, for example semi-transparent perovskite on silicon solar cell with interdigitated back contact silicon bottom cells tandems reaching 33.9% [3] potentially exceeding the Shockley-Queisser limit [4]. Educational aspects of perovskite solar cells have firstly been described aimed for undergraduate chemistry students using drop coating and routine equipment for material deposition by Padwardhan *et al.* [5].

Perovskites crystallise in a calcium titanium oxide mineral (CaTiO<sub>3</sub>) ABX<sub>3</sub>-like structure, where A is methyl ammonium iodine (CH<sub>3</sub>NH<sub>3</sub>PbI<sub>3</sub> MAI), B is lead (Pb) and X is iodine (I). The inorganic framework consists of BX<sub>6</sub> octahedra with A cations occupying the voids. So far, the best results in photocurrent and photovoltage are optimized by mixing different A and X ions simultaneously. Major drawbacks so far have been that perovskites contain lead, which is harmful to the environment especially in its ionic form Pb<sup>2+</sup> (which is a bigger problem than Cd in CdTe because of the lower chemical stability of the material) and the stability of the material and lifetime of carriers. Hence, suitable precautions have to be taken and safety regulations of the university lab for handling of lead compounds in an educational lab considered. Currently, lead containing perovskite solar cells show much higher efficiencies than materials with e.g., ionic tin (which is harmful too) [6]. However, PV modules are currently not part of the Ordinance on the Avoidance of Lead in the Production of Electronic Equipment (RoHS).

This work summarises the interim results of a university course that was held over 5 semesters in a basic teaching lab without major adaptations such as inert gas techniques for 3<sup>rd</sup> year engineering students of eco-energy engineering (OET)/ applied energy engineering (AET) at the Upper Austrian University of Applied Science. It is aimed to train students in photovoltaics and its emerging technologies, basic chemistry, material science, project management, scientific working and presentation and characterisation methods such as Scanning Electron Microscopy (SEM) and solar cell characterisation. Each group spent a day of excursion at the Fraunhofer Institute for Solar Energy Systems (ISE), where students were able to discuss their early results and new ideas with researchers active and well known in the field [7,8]. Though the comparison of their own with latest results, students were able to question and adjust their own research approach developed throughout the course. Preliminary results of this project have been presented at International Symposium of Renewable Energy Education (ISREE) meetings in [9,10]. This paper is based on unpublished results of student reports of reportwinter14 [11], reportsummer15 [12], reportwinter15 [13], reportsummer16 [14], reportwinter16 [15] and describes comprehensively and in more detail the preparation of perovskite solar cells produced by a two-step

process as described in Burschka *et al.* [16] adapted to a teaching lab. Copper thiocyanate (CuSCN) is used as hole transport material, while expensive spiro-OMeTAD is avoided. The active material is deposited by an in-house built spin coater and dried by an in-house built vacuum vessel ('Pressure'), while solar cell testing is done with an improvised solar simulator and solar cell characterisation.

## 2 Experimental

### 2.1 Structure and Performance of Solar Cells

The perovskite solar cell designs pursued in this work are shown in Figure 1. Similar to a dye sensitised solar cell [17] the absorber material perovskite is hosted by a titania (TiO<sub>2</sub>) scaffold. When light is absorbed in perovskite a photogenerated electron is transferred to n-type TiO<sub>2</sub>, while the extracted hole is conducted by p-type material such as spiro-OMeTAD or the low-cost alternative CuSCN and via the electrode to the connected circuit.

All solar cells used FTO (fluorine doped tin oxide, SnO<sub>2</sub>:F) as substrates, which are further described in subsection 2.2. Figure 1a shows the structure of design A (reportwinter14) [11] based on Liu *et al.* [18]. In this design the FTO coated substrate was etched before titania deposition (refer to subsection 2.2). The solar cell consists of a TiO<sub>2</sub> scaffold that hosts the perovskite and CuSCN instead of spiro-OMeTAD as p-type conductor and a gold foil back contact (refer to subsection 2.3 for more details on deposition of materials). Figure 1b shows structure B (reportsummer15) [12], where FTO is followed by a titania scaffold that hosts perovskite and the hole-transport material CuSCN that forms the pn-junction and uses graphite coated FTO glass as back contact. Figure 1c shows design C the structure pursued in (reportwinter16) [15], where FTO coated glass is coated with titania-scaffold hosting the perovskite and is masked (and stayed masked) before a layer of CuSCN is deposited and graphite (or silver paste) is used as a back contact. In this case, mechanical impact can be reduced since only one single glass contact coated by graphite and silver paste is used.

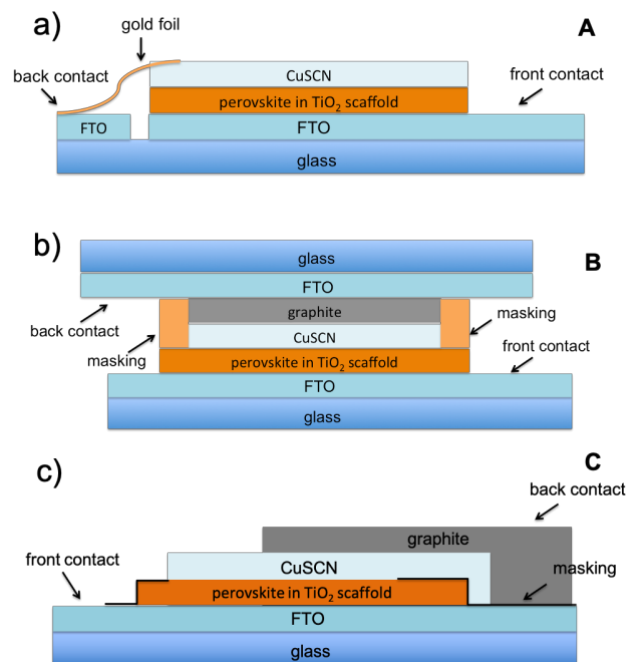


Figure 1 The structure of different the perovskite solar cells a) Design A (reportwinter14) [11] suggests etching the FTO layer and uses gold foil as back contact b) Design B (reportsummer15) [12] after depositing titania/perovskite and CuSCN uses graphite and FTO glass as back contact c) the structure of design C (reportwinter16) [15] shows the lowest mechanical impact by using just one FTO coated glass coated with titania/perovskite and CuSCN graphite and/or silver paste.

The solar cells are characterised by their open circuit voltage ( $V_{OC}$ ) and short circuit current ( $I_{SC}$ ) measured by a Fluke 189 True RMS Multimeter.

The  $V_{OC}$  was ranging between 150-800mV and the  $I_{SC}$  up to 350mA, depending on cell size and irradiation in the range of 800-1100 W/m<sup>2</sup>. The overall cell performance is rather low, below 1%, mainly because of limited time during the course. Table 1 lists the results in greater detail. All results were obtained with the described

shortcomings of the sun simulator measurement in subsection 3.3. Hence, solar cell performance is expected to be higher with better measurement conditions.

**Table 1.** Solar cell performance of different solar cells

Design	$V_{OC}$	$I_{SC}$	Irradiation /W/m <sup>2</sup>	Efficiency	Source
A	500mV	20-50 $\mu$ A	800		Reportwinter14 [11]
B	860mV	356mA	1100	0.39% (0.72cm <sup>2</sup> )	Reportsummer15 [12]
B	200-800mV	50-350 $\mu$ A	800-1100		Reportwinter15 [13]
C	200-800mV	100-350 $\mu$ A	800-1100	0.39%	Reportsummer16 [14]
C	150mV	20 $\mu$ A	800-1100		Reportwinter16 [15]

## 2.2 Substrate and Masking

For the safety of the solar cell as well as the student's health substrates should be touched with gloves at all times. Commercially available FTO (fluorine doped tin oxide, SnO<sub>2</sub>:F) coated glass, which is electrically conducting on one side, heat resistant, and has transmittance properties in the required wavelength range is used as a substrate and is shown in Figure 2. Firstly, the material is cut in 4x4cm<sup>2</sup> square pieces as shown in Figure 2a). Organic and inorganic contamination is removed by putting the substrate in distilled water and an ultrasonic bath for 5 min, and rinsed with acetone afterwards. For the future identification of the substrates consecutive numbers are engraved in all pieces.

Before the materials that form the solar cell are deposited, the surface has to be masked. A recommended masking tool is Kapton tape, which is stable over a wide temperature range and leaves no residue as commercial (or better Scotch) tape shown in Figure 2. Masking has to be applied firmly and without pinholes, gaps or openings. Even the thinnest gap in the masking can lead to a shortcut possibly destroying the cell. Masking is performed after every layer of a material deposition. It is advised to mask smaller after each step.

To avoid short circuit, it may be beneficial to separate the back and the front contact are separated by etching with zinc and hydrochloric acid for the solar cell design A shown in Figure 1a (reportwinter14) [11]. In Figure 2b the substrate is masked and an aqueous zinc powder slurry is put to the area where FTO should be removed. By adding a few drops of 2 molar hydrochloric acid the acidic reaction leads to the release of hydrogen gas. The process is repeated until the ohmic resistance is a few kilo ohm. The cell is rinsed and cleaned again with acetone and ethanol. To block the contact between the front and the back contact a few drops of thioacetamide (TAA) were put on the etched groove and the cells are heated at 500°C for 30 minutes in air. Adding the blocking layer results in a higher resistance. Figure 2c and 2d show the substrate masked with tape and marked.

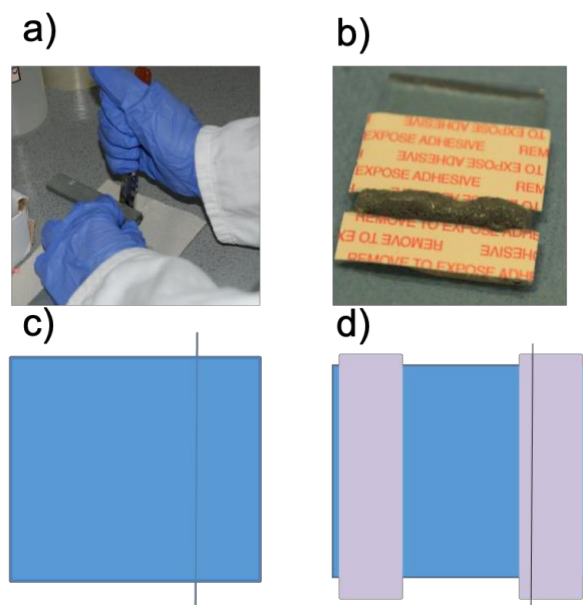


Figure 2 a) Cutting FTO coated glass into 4x4cm<sup>2</sup> substrates with a diamond glass cutter and a ruler. b) The substrate is masked with commercial tape and etched with zinc and hydrochloric acid to separate back and front contact. c) Schematic of the etched substrate d) Schematic of the etched substrate masked with Scotch tape or Kapton (preferred) tape for TiO<sub>2</sub> deposition.

### 2.3 Solar Cell Production Process

Figure 3 shows the work place for the cell fabrication that is installed in a fume hood for safety reasons. It is equipped with two hot plates and the in-house built spin coater (for a more detailed description refer to subsection 3.1) as shown in Figure 3a and 3b. The chemicals are prepared under another fume hood to be supplied to the work place when needed. Before spin coating the materials, the substrates surfaces are wetted with the to-deposited material in solution using a pipette shown in Figure 3c and 3d.

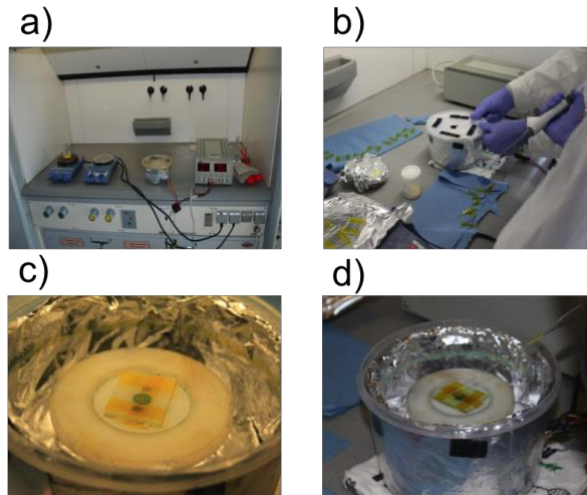


Figure 3 Setup of the first spin coater: a) Work place in fume hood with spin coater and two hot plates. b) The spin coater is closed with a lid during rotation. c) Mounting of the solar cell substrate. d) For material deposition a 5-10 drops of material in solution are used to wet the substrates surface.

#### 2.3.1 Preparation of the Titania Scaffold

To create a suitable and n-type conducting titania scaffold capable of hosting the perovskite absorber a solution of titaniumdiisopropoxide bis(acetylacetonate) and ethanol (1:4) (Sigma Aldrich) is used based on the process described in [7,8]. The masked substrates shown in Figure 4a are wetted with 5-10 drops as shown in Figure 3d and spin coated. After drying at 125°C for 10 min, the films are gradually heated to 500°C in a muffle furnace (shown in Figure 4b) and left at this temperature for 15 min before cooling down to room temperature. Prior to use they are again dried at 500°C for 30 min as described in [16]. A dried titania coated substrate is shown in Figure 4c. The gap that can be seen here too is created by etching as described in subsection 2.2.

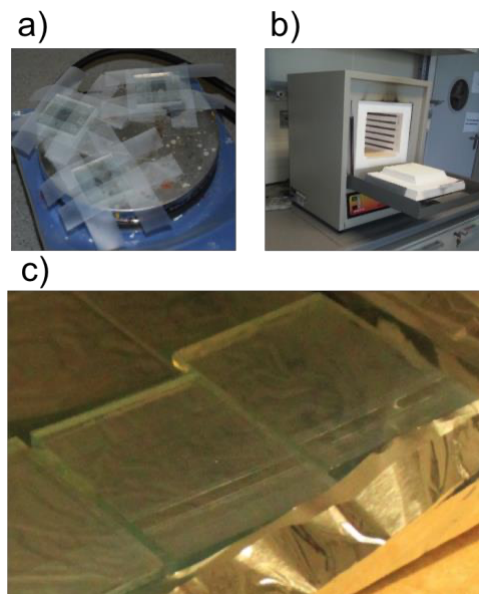


Figure 4 a) Scotch tape masked solar cell substrates on hot plate b) A high temperature muffle oven c) The (etched) solar cell substrates coated with the  $\text{TiO}_2$  scaffold.

### 2.3.2 Preparation of the Perovskite Absorber

The approach to produce the perovskite absorber used in this work is a two-step-based deposition procedure described by Burschka *et al.* [16]. To prepare a solution of 1 ml 0.5 mol of dry  $\text{PbI}_2$  is needed. Lead diiodide is dried in the in-house built vacuum vessel 'Pressure' (described in greater detail in subsection 3.2) before dissolved in N,N-Dimethylformamide (DMF) at  $70^\circ\text{C}$  under constant stirring as shown in Figure 5a. The  $\text{PbI}_2$  does not dissolve completely, and after the residue settles the supernatant is extracted with a pipette. About 5-10 drops of supernatant are used to wet the substrate, which is kept at  $70^\circ\text{C}$ . The  $\text{PbI}_2$  solution is kept at  $70^\circ\text{C}$  for later use. The solar cell substrates are kept at  $70^\circ\text{C}$  for 30 min and the spin coater is run for 90 s at 2500 rpm (at maximum speed) and dried at  $70^\circ\text{C}$  for 30 minutes (as shown in Figure 5b). The best results for solar cell performance are found for substrates pre-heated at  $70^\circ\text{C}$  before material deposition.

The perovskite structure  $\text{CH}_3\text{NH}_3\text{PbI}_3$ , crystal structure ( $\text{ABX}_3$ ), forms, when  $\text{PbI}_2$  and methyl-ammoniumiodide (MAI,  $\text{CH}_3\text{NH}_3\text{I}$ ) react. Therefore, the  $\text{PbI}_2$  hosted in the titania scaffold is dipped in a solution of 1g  $\text{CH}_3\text{NH}_3\text{I}$  in 2-propanol (2-isopropanol) for 20 s to start the reaction, then rinsed with 2-propanol and finally dried at  $70^\circ\text{C}$  for 30 minutes. During this procedure, the reaction can be clearly seen by the change of the colour from yellow to a dark brown depicted in Figure 6a-c. The resulting colour depends mainly on the thickness of the light absorbing material (refer also to Figure 5c and 5d). Since  $\text{CH}_3\text{NH}_3\text{I}$  (MAI) powder is sensitive to humidity, exposure to atmosphere is kept as short as possible and the material is dried using e.g., the device 'Pressure' (refer to subsection 3.2).

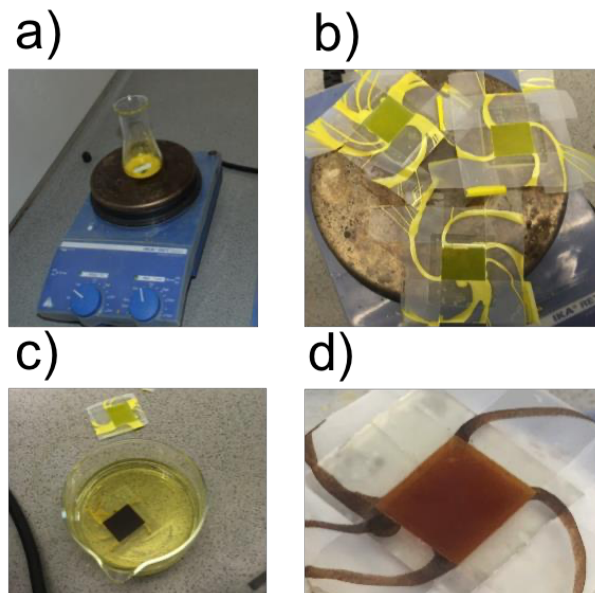


Figure 5 a)  $\text{PbI}_2$  solution in N,N-Dimethylformamide (DMF) b)  $\text{PbI}_2$  after spin coating and hosted in the titania scaffold of the solar cell substrate c) The formation of perovskite (brown) coated  $\text{PbI}_2$  while dipping in MAI d) Perovskite hosted in titania scaffold after drying.

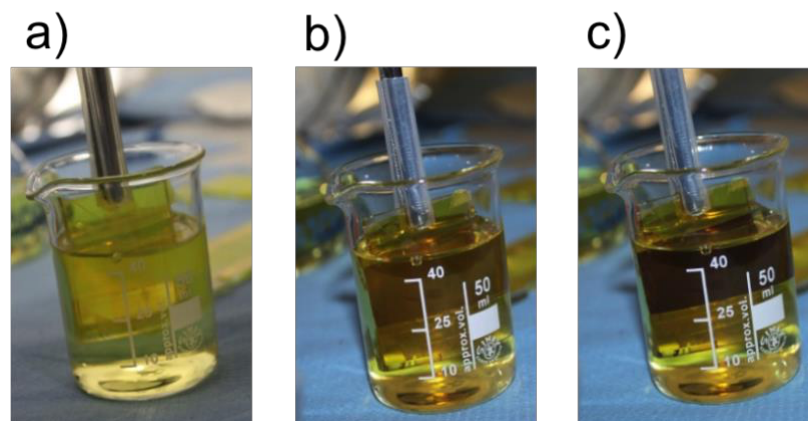


Figure 6 a-c) Change of the colour when perovskite is formed during the dipping process within 25 seconds. Note: the yellowish colour of methyl-ammoniumiodide (MAI) is a sign of degradation and should be avoided.

### 2.3.3 Deposition of Hole Transport Material Copper-Thiocyanate (CuSCN)

Copper-thiocyanate (CuSCN) is used as low-cost hole-transport material (HTM). For preparation of the solution 200 mg of CuSCN are dissolved in 8ml dipropyl-sulphide and kept in an ultrasonic bath for one minute. Then another 2 ml dipropyl-sulphide are added and the solution is ultrasonicated for another minute. Before use, it is put in a common refrigerator for 24 hours and stored there whenever not needed. The solution is saturated and solid residue settles at the bottom. The hole-transport material is then created by dropping 5-10 drops of the supernatant to wet the substrate and to spin coat at about 4000 rpm for 30s. The resulting solar cell is dried at 80°C.

### 2.3.4 Back Contact of Solar Cell

Perovskite is heat sensitive above 80°C. Hence, the contact has to be realized without a high temperature process. A suitable contact between the hole transport material and the back contact is needed to characterise the solar cells sufficiently. Cheap and simple low temperature solutions involve gold foil, graphite of various grain sizes, as well as commercial silver paste. Gold foil used in design A Figure 1a (reportwinter14) [11] for example can be tricky to apply since it exfoliates and detaches easily as shown in Figure 7a and 7b. Graphite on the other hand tends to scratch and destroy the underlying structure, and commercially available silver paste may cause unwanted chemical side reactions.

In order to find a suitable back contact, the whole design of the cell had to be adapted during the project. Gold sputtering (as in SEM sample preparation) has also been tried, but is not practical. Copper cello tape turned out not practical too. As a result, graphite powder attached to a counter FTO- glass plate was used most of the time.

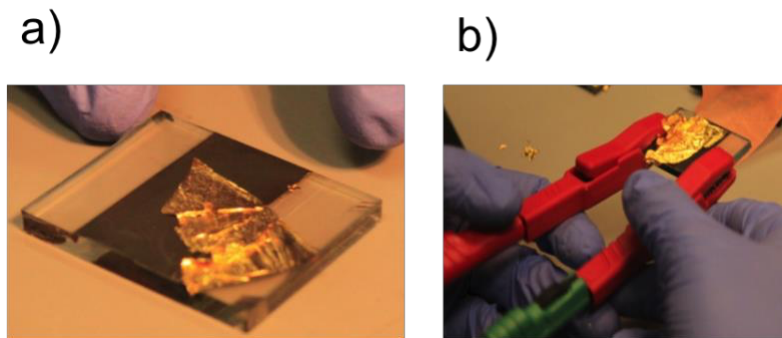


Figure 7 a) Gold foil contact b) Connection of gold foil to the measurement device.

The best result in the design B in Figure 1b (reportsummer15) [12,13], however, was received with a graphite powder dispersed in isopropanol<sup>1</sup> into a high viscosity paste. The paste is dropped on the CuSCN layer and further contact made with the conductive side of another FTO-glass. To avoid short circuit as well as destruction of the cell the masking (for the CuSCN) layer was often not removed such as in the solar cell design C of Figure 1c (reportwinter16) [14,15], where contact was made with a graphite in isopropanol slurry.

### 2.4 Material Characterisation

The performance of solar cells depends also on the absorption depth and hence the layer thickness to enable a sufficient absorption of photons as well as the diffusion length of charge carriers. The diffusion length describes the average way of a free charge carrier until its recombination. A short diffusion length reduces the cell performance with rising layer thickness. The thinner the layer, the less charge carriers are recombining before reaching the contacts. Hence, the perovskite is embedded in a TiO<sub>2</sub> dense scaffold and in high performance cells perovskite cells this absorber layer is optimized to a thickness of about 350 nm [19,20]. Therefore, for a low transmitting irradiance of about 2% ( $\frac{E(x)}{E_1} = 0,02$ ) is perovskite layer with an absorption coefficient of about  $\alpha = 10^5 \text{ cm}^{-1}$  should be at least  $x = 391.2 \text{ nm}$  thick for this work.

The layer thickness is measured via the cross section of the tested solar cells shown in Figures 8a and 8b were measured in the Scanning Electron Microscope (SEM) and shows a cell thickness of around 1300 nm. The cubic structure along with the defects of perovskite are shown in Figures 8c and 8d. Due to the limited possibility to

---

<sup>1</sup> Ethanol for example is hygroscopic and may react with perovskite; hence isopropanol was used to disperse the graphite.

protect the cell from dust during the production process on air impurities, one can expect to detect impurities in the material, which can cause a decrease the overall cell performance. This effect, however, is even more significant in thinner layers.

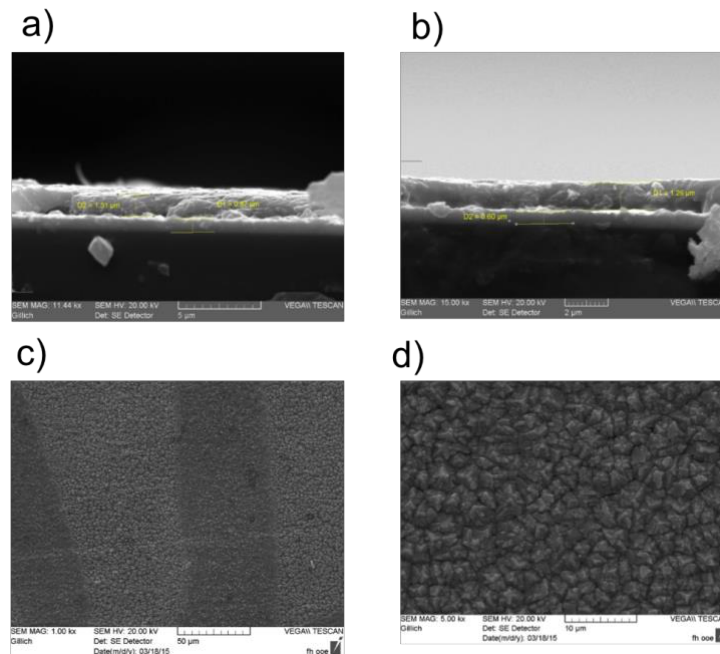


Figure 8 a) SEM analysis, cross section. The scale bar is 5 μm. b) SEM analysis cross section. The scale bar is 2 μm. c) SEM analysis surface. The scale bar is 50 μm. d) SEM analysis surface. The scale bar is 10 μm.

To produce cells with less defects, the cell size was reduced radically from 5 cm<sup>2</sup> to less than 1 cm<sup>2</sup> over project time. In the measured results the relation between the cell size and the failure rate is evident and shown in Figure 9 (reportwinter15) [13], where cell design 1b investigated a correlation between size (0.5-6cm<sup>2</sup>) to voltage 0.7-0.01V.

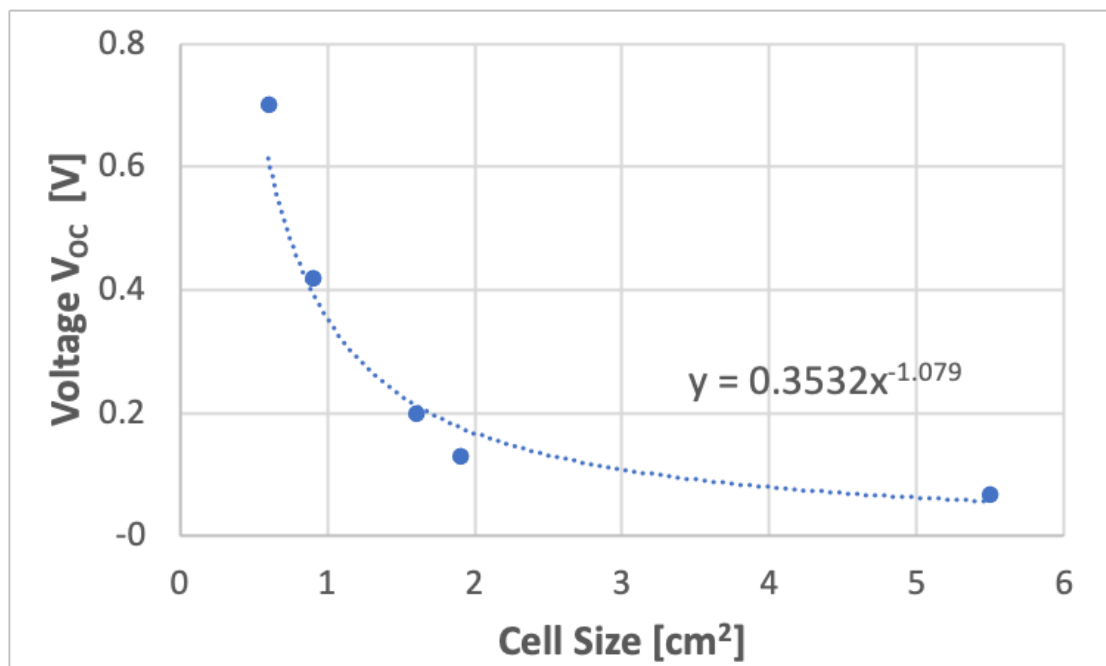


Figure 9 Correlation of cell size and voltage (reportwinter15) [13].

## 2.5 Use of Social Media during Project



The group of reportsummer15 [13] has produced a video during preparation ‘Inorganic- Organic Perovskite Hybrid Solar Cell’, which was published on YouTube [21] describing the production process along with footage of work done in the lab.

### 3 In-House built Lab Equipment

#### 3.1 In-House built Spin-Coater

Preliminary experiments, where drop coating and spin coating are compared to find a suitable process for  $\text{TiO}_2$  and  $\text{PbI}_2$  deposition are shown in Figure 10. The results demonstrate that deposition of  $\text{PbI}_2$  with an in-house built spin-coater as in Figure 10b produces thinner and more homogenous material than drop coating as in Figure 10a. It was found that a spin coating process is suitable to deposit materials such as  $\text{TiO}_2$ ,  $\text{PbI}_2$  and  $\text{CuSCN}$  more homogeneously. The reduced layer thickness also decreases the internal resistance of resulting solar cells and is hence expected to show better results.

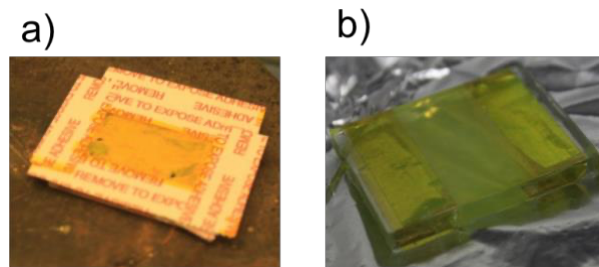


Figure 10 a) Drop coating of  $\text{PbI}_2$  vs. b) Spin coating of  $\text{PbI}_2$ . Spin coating shows a more homogeneous surface than drop coating.

The first spin in-house built spin coater is shown in Figure 11 (and Figure 3) uses a common modelling electric motor put it into a cylindrical box made out of PE (a common gummi bear box), which can be closed by a lid (reportsummer15) [13]. The inside of the box is wrapped with aluminium foil so that harmful chemicals can be removed from the spin coater after use. On the rotating part of the motor a milled plastic slice is put where the substrates can be mounted. A three-phase-motor is installed and controlled with a Speedstar BRUSHLESS Crawler Robitronic Controller (S040012C) in combination with a Servo Tester. The circuit as shown in Figure 11b is supplied by a DC power source (TTi CPX200 DUAL 35V 10A PSU). This spin coater is able up to rotate up to 5000 rpm and can be regulated by voltage.

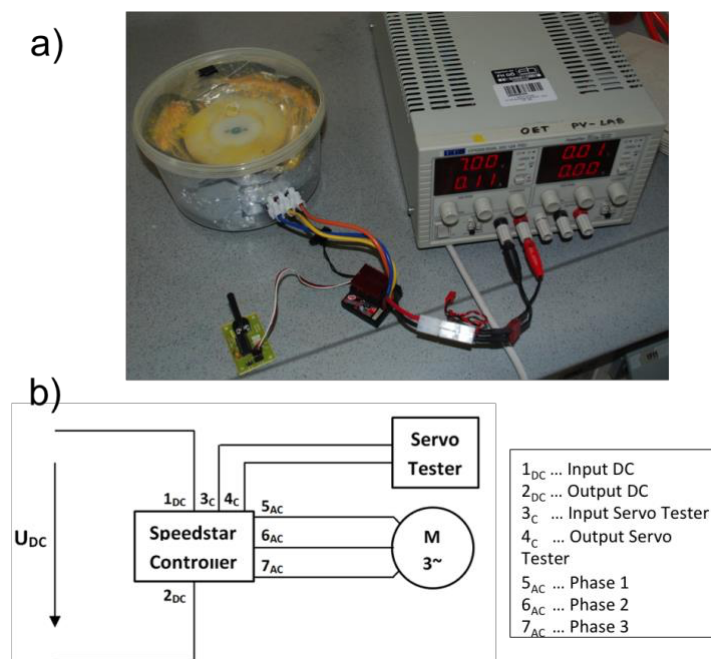


Figure 11 a) In-house built spin coater and control system b) Circuit of in-house built spin coater (reportsummer15) [13].

In this work two different procedures are used. At low engine speed of  $1500 - 2000 \frac{1}{min}$  and at 3.5V and 1A

DC and at high engine speed in the range of  $2500 - 3000 \frac{1}{min}$  at 7V and 1.75 A DC. The spin coater is later (reportwinter15) [14] updated and the design changed in a way to protect the motor to prevent chemical corrosion. As a result, the motor is now outside the plastic box as shown in Figure 12. Figure 12a shows the constructional sketch. To increase the working comfort an aluminium plate is added on the rotating plate with a recess in the middle in which the substrate is put for material deposition. Additionally, a massive steel bottom plate is added to increase the stability and to reduce vibrations. The overall setup is shown in Figure 12b and the close up of the sample holder in Figure 12c. This update allows an increased rotation speed and finer adjustment as well as increased safety.

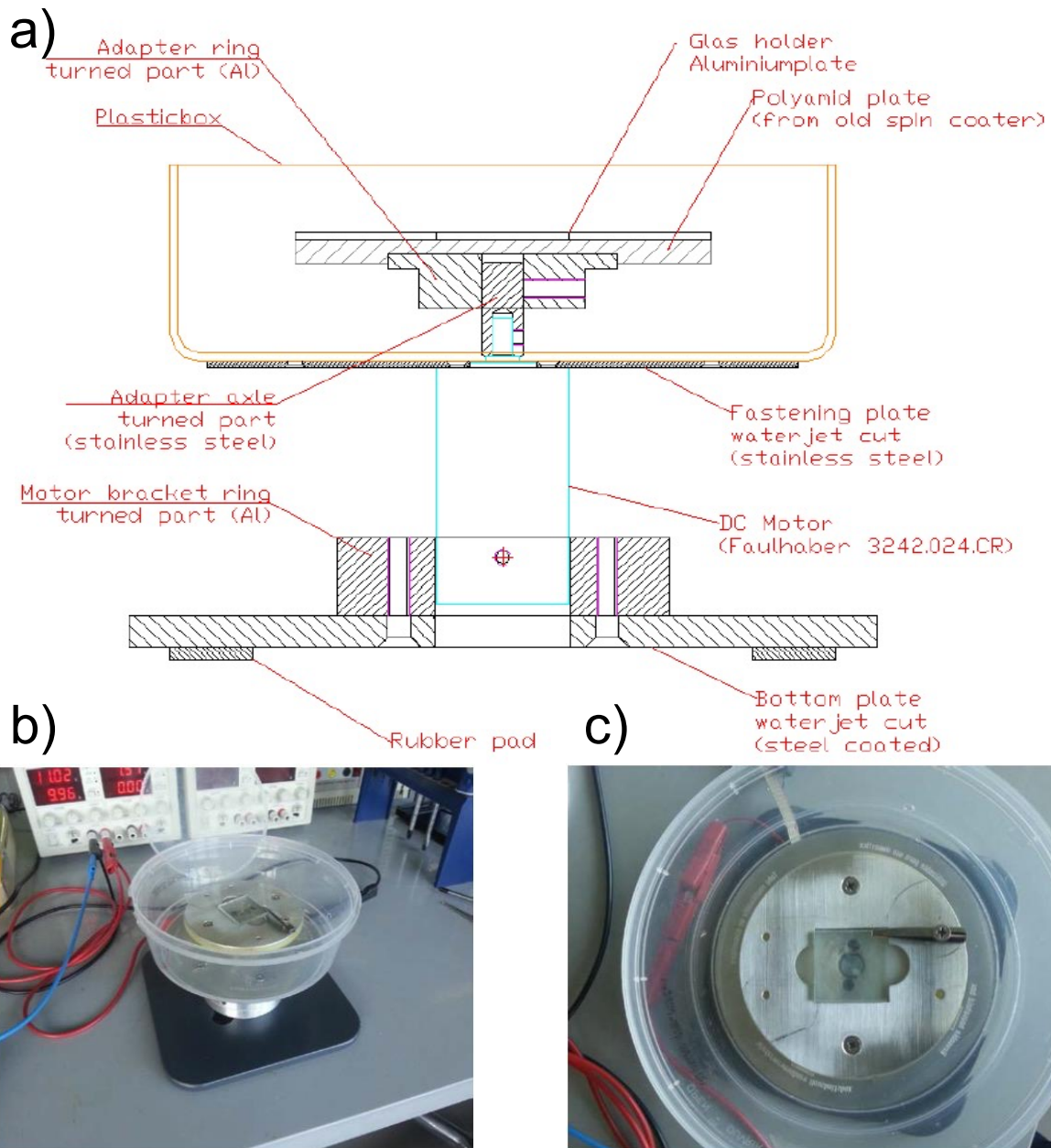


Figure 12 a) Schematic design of updated spin coater b) updated spin coater and set up c) Close up of sample holder (reportsummer15) [13].

The required voltage has to be determined by metering the value in the diagram in Figure 13. An added trend line of the linear equation of the motor characteristic shows that the measured motor constant is smaller, but quite close to the value given by the manufacturer. This voltage is then adjusted on the laboratory power source (using a voltmeter for high accuracy). The motor used is a Faulhaber 3242 024 CR, a DC-motor with 5300 rpm idle speed at 24 V nominal voltage and 26.3 W output power. This type of motor is easily cable-connected with a DC voltage source, which provides a direct correlation between the electric supply voltage and the rotation speed

with an accuracy of at least +/- 50 rpm. The rotational speed constant for this motor is 231 rpm/V. The supply voltage multiplied with this constant gives the rotational speed of the motor. To ensure a high accuracy of the rotational speed, the relation between the voltage and the rotation speed is measured in steps of 5 V for this motor with a contactless Testo rpm kit.

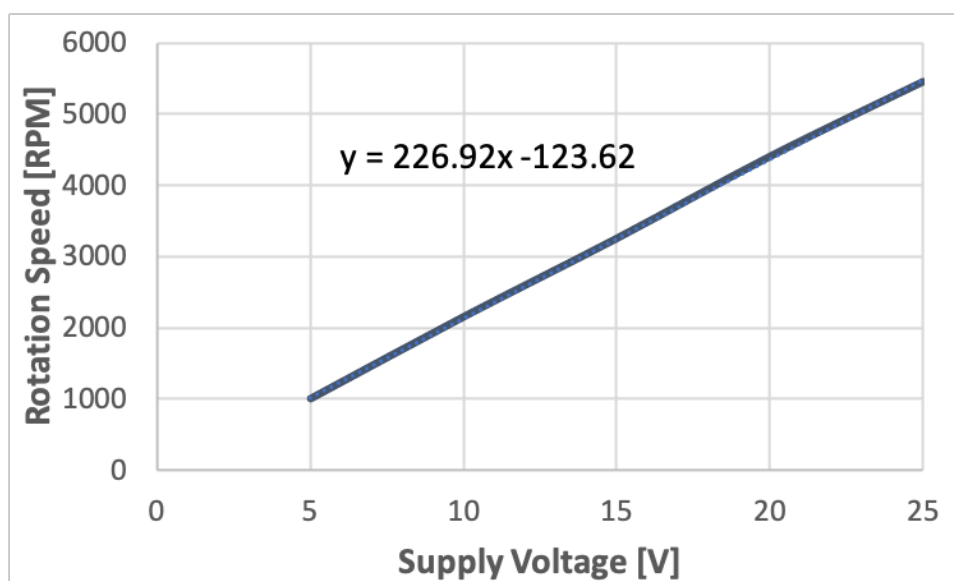


Figure 13 Rotation speed vs voltage motor characteristics of updated spin coater

### 3.2 'Pressure' - a Vacuum Vessel to Dry Chemicals

Perovskites are sensitive to humidity so dry materials have to be used throughout the process. Both,  $\text{PbI}_2$  as well as MAI have to be dried before reaction. Furthermore, MAI evaporates at a temperature of 150 °C. 'Pressure' is an in-house build device designed to dry chemicals is an air-tight cubic, which can be filled with nitrogen or hold a vacuum and is shown in Figure 14 (reportsummer16) [14]. A block of aluminium with 650mm x 650mm is used as raw material (refer to Figure 14a). To store material a hole with the diameter of 360mm is milled in the middle of the aluminium block (refer to Figure 14b). Two more holes are milled from the outside to the centred middle hole. One of these holes is for the valve (Figure 14c), which is needed to fill with nitrogen. This valve that is taken typically for the tires of a motor-lorry. It holds pressure of about 10bar, which is sufficient, because the maximal pressure of the nitrogen in the aluminium block is 2bar. The other hole is the pressure relieve valve. For this valve that is normally used for the nitrogen pressure cylinder of a pressure reducing regulator (SK 265-004), with a range of 0-7bar is chosen.

To test 'Pressure' dry silica gel (tried overnight at 80°C) is put into two beakers of the same size. The mass of each filled beaker glass is measured before and after 25.5 h and 52 days, respectively. One beaker glass is put in 'Pressure' that is filled with nitrogen and the other beaker glass is left in atmosphere. Dry silica left in 'Pressure' gained 0.12wt% after 25.5 h and 0.61wt% after 52 days, respectively. When left in atmosphere the mass of the gel increased by 3.1% after 25.5 h and 29.9% after 52 days though humidity (refer to Table 2), respectively. When the pressure relieve valve pulled nitrogen is released proving the sealing lasted for up to 52 days. In both cases the silica gel has nearly the same colour as on day one when it was dry, which is orange and shown in Figure 15.

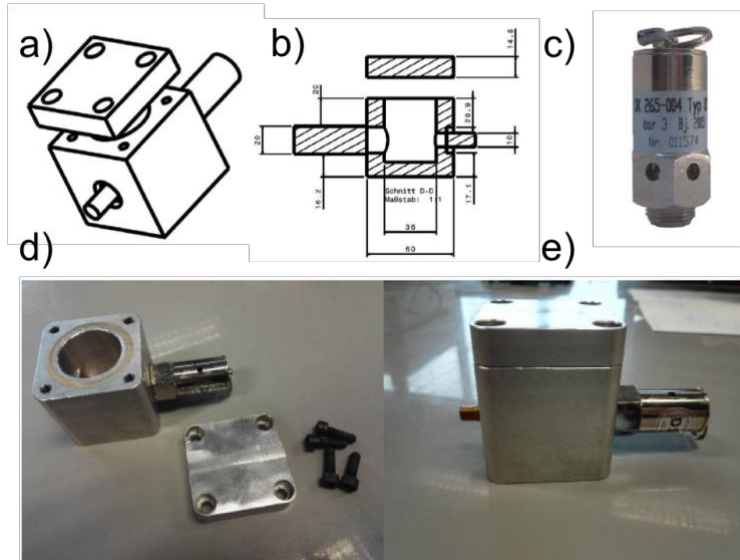


Figure 14 'Pressure' concept a) b) schematic c) valve used to contain nitrogen d) device open e) device sealed (reportsummer16) [14].

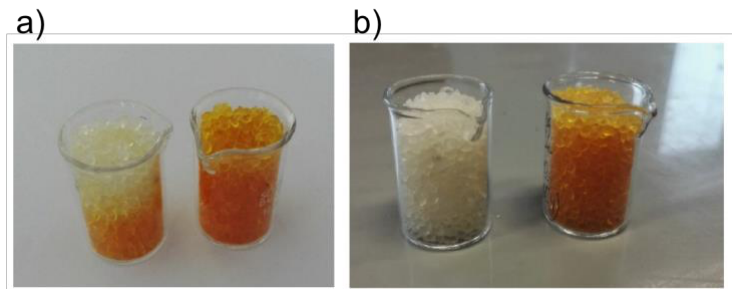


Figure 15 Left glass: gel in atmosphere, right glass: gel in 'Pressure' a) Short term test for 25.5h b) Long term test for 52 days. An orange colour indicates dry material. The colour of the gel changes to white when exposed to humidity.

**Table 2.** 'Pressure' performance short and long-term test.

	Mass/g day 1	Mass/g after test	Difference %
Silica gel ('Pressure')	9.1656	9.1775	0.1296
Silica gel (atmosphere for 25.5h)	8.6529	8.9229	3.131
Silica gel ('Pressure')	9.1775	9.2210	0.611
Silica gel (atmosphere for 52d)	8.9229	11.236	29.876

During the preparation of perovskite solar cells the silica gel shown in Figure 15 is also used for the drying process. For example, MAI or  $PbI_2$  and the silica gel is put in 'Pressure' and into the muffle furnace at 80 °C to speed up the drying process.

### 3.3 In-House built Improved Sun Simulator and Solar Cell Characterisation

The perovskite solar cells are characterised using an in-house built and improvised solar simulator equipped with a halogen lamp normally used in a sun simulator for solar thermal characterisation (reportsummer14) [11]. The purple line in Figure 16 shows the radiation spectrum of the used lamp compared with the blue line representing the AM1.5 spectrum and the red line showing perovskite absorption under AM1.5 irradiation. The purple line in Figure 16 shows a peak at 630 nm, when the lamp is supplied with 17V. In this case the maximum of the radiation is already shifted significantly to the infrared radiation range compared to the AM 1.5 spectrum.

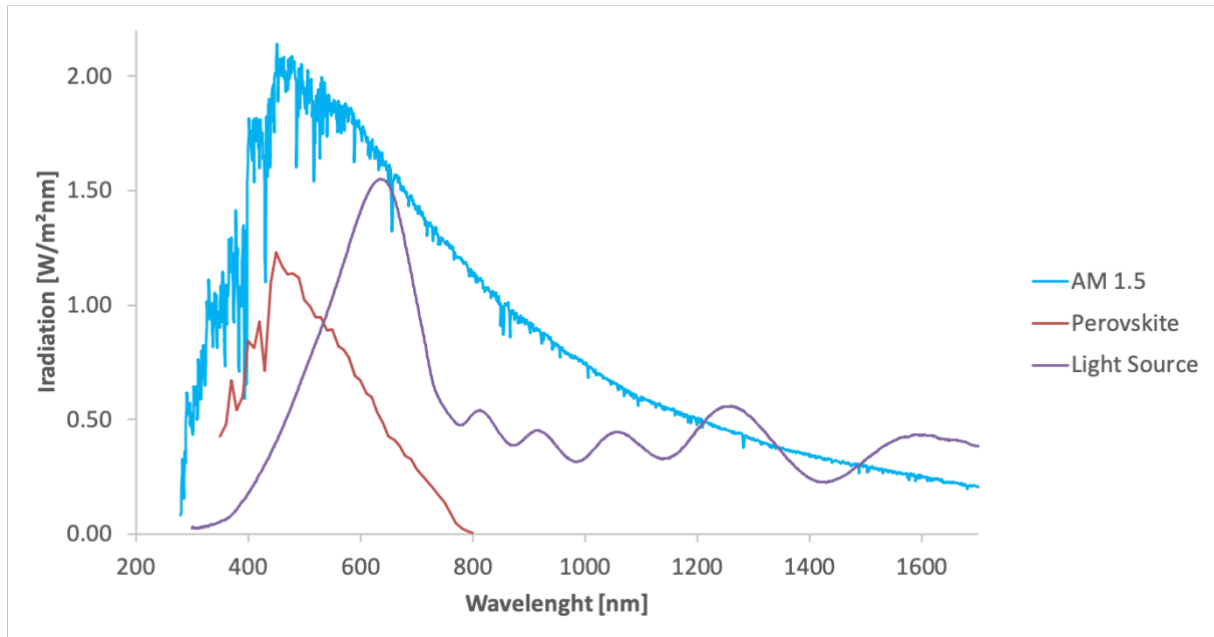


Figure 16 a) Radiation spectrum of halogen lamp (ASiC Wels), AM1.5 and cell performance under AM 1.5 irradiation

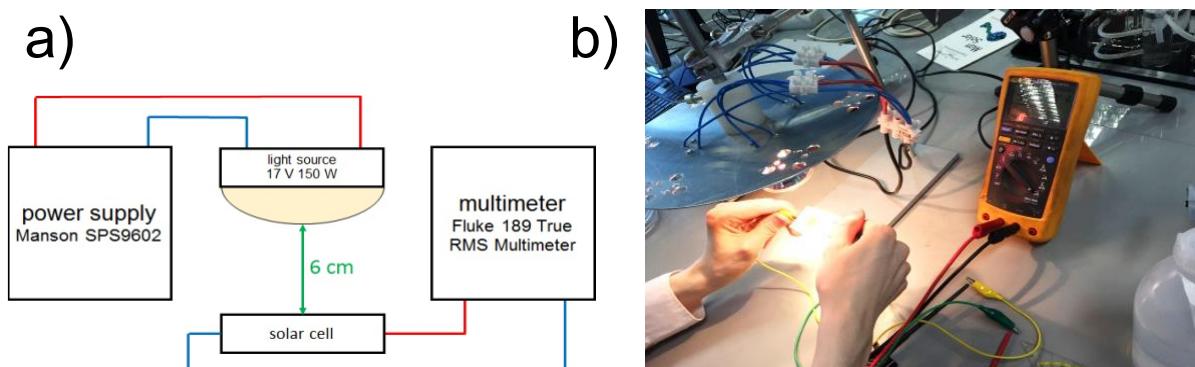


Figure 17 a) Schematic diagram of the test setup b) Test set-up for solar characterisation.

Figures 17b and 17c show the test-setup and its schematic diagram, which is used to test the perovskite solar cells. A Manson SPS9602 power supply was used to power the halogen lamp with a voltage of 9.5 V to get a radiation of  $1100 \text{ W/m}^2$  at a distance of 6 cm. This means that the spectrum in which the cells are tested is even more displaced to the infrared spectrum according to Wien's displacement law.

Additionally, the irradiation of the lamp was measured with a silicon sensor. Due to the lower bandgap of 1.12 eV the silicon measures radiation up to 1200 nm. The bandgap of perovskite is 1.55 eV and as a result light with a wavelength range above 800 nm does not contribute to the cell performance since energy of this radiation is not sufficient to cross the bandgap. This means, that major parts of the measured radiation under which the perovskite solar cells are tested, cannot contribute to the actual cell performance. Furthermore, the incident-photon-to-current-rate (IPCE) is already very poor at a range of 600-800 nm as a result from the weaker absorption of the perovskite in this spectral region as described in [16]. Thus, the measured cell efficiency under a light source according to the AM 1.5 spectrum is expected to be significantly higher.

For an improved measurement, however, it is also advisable to use a LED-lamp should be used instead of a halogen lamp to avoid overheating, which also affects the measurement.

#### 4 Discussion and Teaching Experiences

High performance cells are reported to be produced in a controlled atmosphere and were sealed to protect the cell. This work, however, was done under limited time (30h per semester) and limited costs (1000€) and is intended to serve as an inspiration how to teach cutting edge research topics such as perovskite solar cells in a basic teaching lab. This course-project has been an entry not just into the production process of a solar cell, but also in a development of research project with project management process with an unknown outcome. Although

there was a good working basis through the project documentation of the previous groups, lots of new questions and problems arose while working on the problem. Every new step, which was made had to be validated by trial and error and then documented accurately, using the scientific method.

Perovskite solar cells are an emerging technology with one record efficiency beating the other. So, from a supervising point of view it was quite easy to get students motivated. However, the overall topic is complex and difficult to grasp for undergraduates, especially in the short time available. Discussions with active and known researchers and visit active research labs such as those at ISE Freiburg has proven extremely helpful to underline the importance and actuality of the research topic and gave students the opportunity to adjust their own research approach based on latest research results. Furthermore, the presentation of own results in the form of poster presentations, reports and a YouTube video motivated students to beat last year's results.

Generally, work has to be as clean and dry and safe as possible. A reduction of the perovskite and other layer thickness causes an increase of the cell efficiency. However, when using simple lab techniques as here, a decrease in thin film thickness might also lead to an increase in defects. Another point of consideration is that the cells must not be exposed to humidity in any form. Better overall results with the equipment available, however, were found with the two-step method (instead of using a pre mixed commercial solution).

The in-house build devices such as the spin coater, 'Pressure', and the improvised sun simulator were designed on limited time and resources. Time was often too short to really improve changes on the design and as result material quality and resulting solar cell efficiencies stayed very low. However, some of the students involved in this project do now pursue careers in perovskite research.

## Acknowledgements

This work did not receive any specific grant from funding agencies in the public, commercial, or not for profit sectors.

Many thanks to the students involved in this project: Florian Pfeffer, Valerie Rodin, Martina Grubmüller, Johannes Schmiedhuber, Florian Bamberger, Stefan Breitwieser, Christian Buchegger- Kranawetter, Franz Diermair, Florian Mayr, Christine Sonnleitner, Peter Spitzauer, Sebastian Steinlechner, Rudolf Krenner, Martina Reisner, Thomas Flath, Marjan Kolak, Daniel Moser, Christoph Steiner, Moritz Stiegler, Manuel Hauthaler, Gergely Keresztes, Thomas Peer, Gerold Lehner, Peter Hirner, Tobias Kogler, Patrick Schwarzbauer, Carmen Wagner, Manuel Hautaler, Michael Pamminger, Karim Riezk, Verena Hartinger, Raimund Haslehner, Verena Kaltenberger, Sandra Mitterhuber, Julian Schürz, Erik Stuppacher and Luca Benedek.

Furthermore, the author would like to thank Simone Mastroianni and Gayathri Mathiazhagan from ISE Fraunhofer Institute Freiburg in Germany for providing materials and useful discussions

Michael Steinbatz for financial support, Markus Gillich for the SEM analysis, Helmut Hüttmannsberger and Christian Gruberbauer for their support in the laboratories. Many thanks to Andreas Kirchleitner, who supported the development of the spin coater.

- [1] Kojima, A., Teshima, K., Shirai, Y., Miyasaka, T., Organometal Halide Perovskites as Visible Light Sensitizers for Photovoltaic Cells. *J. Am. Chem. Soc.* **2009** *131*, 6050–6051. <https://doi.org/10.1021/ja809598r>
- [2] <https://www.nrel.gov/pv/interactive-cell-efficiency.html>
- [3] NREL. Best research-cell efficiency chart. <https://www.nrel.gov/pv/cell-efficiency.html>
- [4] Queisser, H.J., Shockley, W., Detailed Balance Limit of Efficiency of p-n Junction Solar Cells. *Journal of Applied Physics* **1961**, *32*(3), 510
- [5] Padwardhan, S., Introducing Perovskite Solar Cells to Undergraduates. *J. Phys. Chem. Lett.* **2015**, *6*(2), 251–255. DOI: 10.1021/jz502648y
- [6] Ibn-Mohammed T., Koh S. C. L., Reaney I.M., Acquaye A., Schileo G., Mustapha K.B., Greenough R., Perovskite Solar Cells: An Integrated Hybrid Lifecycle Assessment and Review in Comparison with Other Photovoltaic Technologies. *Renew. Sustain. Energy Rev.* **2017**, *80*, 1321–1344. <https://doi.org/10.1016/j.rser.2017.05.095>
- [7] Mathiazhagan, G., Wagner, L., Bogati, S., Ünal K.Y., Bogachuk, D., Kroyer T., Mastroianni, S., and Hinsch, A., Double-Mesoscopic Hole-Transport-Material-Free Perovskite Solar Cells: Overcoming Charge-Transport Limitation by Sputtered Ultrathin Al<sub>2</sub>O<sub>3</sub> Isolating Layer, *ACS Applied Nano Materials* **2020**, *3*(3) 2463–2471 doi:10.1021/acsnm.9b02563
- [8] Wagner, L., Mastroianni, S., Hinsch, A., Reverse Manufacturing Enables Perovskite Photovoltaics to Reach the Carbon Footprint Limit of a Glass Substrate. *Joule* **2020**, *4*(4), 882–901, ISSN 2542-4351, <https://doi.org/10.1016/j.joule.2020.02.001>
- [9] Basch, A., Arafa, S., Higher Education and Education of the Public in Energy Conversion in Austria and Egypt Photovoltaics and Electrochemical Storage. *12th International Symposium on Renewable Energy Education*

- Proceedings ISREE 2017*, **2017** 19<sup>th</sup>–21<sup>st</sup> June in Strömstad Sweden 2017  
[http://www.stromstadakademi.se/sa\\_pdf/AAS-33.pdf](http://www.stromstadakademi.se/sa_pdf/AAS-33.pdf)
- [10] Basch, A., Schürz, J., Hartinger, V., Haslehner, R., Kaltenberger, V., Mitterhuber, S., Stuppacher, E. and Benedek, L. Perovskite Solar Cell Lab Course for Undergraduate Engineering Students. *13th International Symposium on Renewable Energy Education Proceedings ISREE 2019*, **2019**, 4<sup>th</sup>–7<sup>th</sup> November 2019 in Santiago the Chile part of Solar World Congress SWC2019 IEA SHC International Conference on Solar Heating and Cooling for Buildings and Industry 2019, doi:10.18086/swc.2019.50.02 Available at <http://proceedings.ises.org>
- [11] Rodin, V., Grubmüller, M., Schmiedhuber, J., Pfeffer, F. Project Report, Perovskite Solar Cells. *Upper Austrian University of Applied Sciences, Student Report Winter Semester*, **2014**, unpublished results
- [12] Bamberger, F., Breitwieser, S., Buchegger-Kranawetter, C., Diermaier, F., Mayr, F., Sonnleitner, C., Spitzauer, P., Steinlechner S., Project Report Organic-Inorganic Perovskite Hybrid Solar Cells. *Upper Austrian University of Applied Sciences, Student Report Summer Semester* **2015**, unpublished results
- [13] Buchegger-Kranawetter, C., Krenner, R., Reisner, M., Project Report Organic-Inorganic Perovskite Hybrid Solar Cells. *Upper Austrian University of Applied Sciences, Student Report Winter Semester* **2015**, unpublished results
- [14] Flath, T., Hauthaler, M., Keresztes, G., Kolak, M., Moser, D., Peer, T., Steiner, C., Stiegler, M., Project Report Perovskite Solar Cells., *Upper Austrian University of Applied Sciences, Student Report Summer Semester* **2016**, unpublished results
- [15] Flath, T., Kolak, M., Moser, D., Steiner, C., Stiegler, M., Project Report Perovskite Solar Cells. *Upper Austrian University of Applied Sciences, Student Report Winter Semester* **2016** unpublished results
- [16] Burschka, J., Pellet, N., Sequential deposition as a route to high-performance perovskite-sensitized solar cells. *Nature* **2013**. 499(7458), 316–319 <https://doi.org/10.1038/nature12340>
- [17] Grätzel, M., Dye-sensitized solar cells. *Journal of Photochemistry and Photobiology C: Photochemistry Reviews* **2003** 4(2) 145–153. [https://doi.org/10.1016/S1389-5567\(03\)00026-1](https://doi.org/10.1016/S1389-5567(03)00026-1)
- [18] Liu, D., Kelly, T. L. Perovskite solar cells with a planar heterojunction structure prepared using room-temperature solution processing techniques. *Nat Photon* **2014** 8(2),133–138. <https://doi.org/10.1038/nphoton.2013.342>
- [19] Grätzel, M. The light and shade of perovskite solar cells. *Nature Mater.* **2014** 13, 838–842 <https://doi.org/10.1038/nmat4065>
- [20] Xing, G., Mathews, N., Long Range Balanced Electron- and Hole Transport Lengths in Organic Inorganic CH<sub>3</sub>NH<sub>3</sub>PbI<sub>3</sub>. *Science* **2013** 342(6156), 344–347 DOI: 10.1126/science.1243167
- [21] Breitwieser, S. Organic – Inorganic Perovskite Hybrid Solar Cell. **2016** [https://youtu.be/z8xG9U\\_0cMs](https://youtu.be/z8xG9U_0cMs)